AUT Journal of Civil Engineering

AUT J. Civil Eng., 6(4) (2022) 509-520
DOI: 10.22060/ajce.2023.22325.5825

Numerical Investigation on Structural Behaviors of Deficient Steel CHS Long Columns Strengthened Using CFRP

O. Yousefi*

Department of Civil Engineering, Nikshahr Branch, Islamic Azad University, Nikshahr, Iran

ABSTRACT: Structures often suffer damage due to various factors, including accidental loads, corrosion, and reduced strength, necessitating the need for repairs. The use of Carbon Fiber Reinforced Polymer (CFRP) to strengthen steel members has gained considerable attention in recent decades. However, most previous research has focused on studying the behavior of non-deficient steel structures. This study aims to investigate long steel circular columns with primary defects in vertical and horizontal notches, and examine the effects of CFRP retrofitting. A total of fifteen specimens of steel long Circular Hollow Section (CHS) columns, each with the same height but varying damage dimensions, were analyzed using ABAQUS 2016 software under compressive load. The main challenge with long columns is global buckling under compressive loads. To improve the accuracy of the analysis, a combined method was employed to study the post-buckling behavior of the plastic zone. Specifically, the specimens underwent elastic buckling analysis followed by RIKS non-linear analysis considering both general and local imperfections. The results showed that defects in the steel columns reduced the load-bearing capacity by up to 52%. Horizontal defects had a greater impact on reducing the ultimate load compared to vertical damage (up to 13%). Additionally, deficiencies significantly affected the buckling of the defect area, resulting in axial deformation. CFRP retrofitting strengthened the columns, increasing the ultimate load capacity (up to 51%), delaying defect buckling, controlling fractures, and reducing stresses in the damaged zone.

Review History:

Received: Apr. 09, 2023
Revised: Jun. 29, 2023
Accepted: Aug. 18, 2023
Available Online: Aug. 23, 2023

Keywords:

Column
strengthening
buckling
deficiency
CFRP

1- Introduction

Most members of structures that have reached the end of their useful life require repair. These members can be damaged by various factors. Due to the high cost of reconstruction and, in some cases, the preservation of historical monuments, a significant portion of a country's development budget is allocated annually for repairing and rehabilitating these structures. Compressive members, such as columns, play a crucial role in bearing and distributing both vertical and lateral loads within a building. The buckling behavior of these elements is of utmost importance and is indicated by a parameter known as the slenderness ratio. Essentially, no column can withstand its maximum capacity and is susceptible to failure caused by buckling. Consequently, many researchers are focused on retrofitting and enhancing column strength through the use of new materials and methods. Although Fiber-Reinforced Polymer (FRP) is a relatively new material and its widespread adoption is still limited, extensive research has been conducted on these materials.

Chen et al. discovered that the inclusion of CFRP sheets enhances the ultimate strength of specimens and effectively delays local buckling [1]. Huang et al. conducted a study on the compressive behavior of steel columns by repairing damaged CHS sections using CFRP or grout. They concluded that both techniques are effective for column rehabilitation [2]. Based on experimental studies conducted by Cinitha et al. it has been determined that corrosion leads to a decrease in steel thickness, mechanical strength, and weight. Furthermore, it has been established that corrosion plays a significant role in reducing the overall capacity [3]. Additionally, Sandrasekaran *et al.* investigated the fracture modes, stress-strain behavior, and ultimate bearing capacity of short steel columns strengthened with CFRP. Their study revealed that as the load increases, the CFRP fibers surrounding the column experience tearing [4]. Wang et al. conducted a study focusing on moderate slenderness columns. In this research, a total of 24 concrete-filled specimens were subjected to axial loading tests. The study findings indicated that failure in columns with small relative slenderness was primarily attributed to low cross-sectional strength. Conversely, for columns with larger slenderness, failure was attributed to column instability [5].

Strengthening of steel columns filled with concrete has been studied extensively. Karimi et al. focused on studying the effects of slenderness on the behavior of steel-concrete composite columns. They conducted tests on a total of nine

*Corresponding author's email: omid.yousefi88@gmail.com

columns and observed that the application of an FRP jacket increased the compressive strength of the concrete by up to 17%. Furthermore, the long composite column specimens demonstrated high stability against global buckling, resulting in an enhanced buckling capacity for long steel columns [6].

Touhari and Mitiche-Kettab conducted an investigation into the behavior of FRP-confined concrete cylinders under compression. The study involved the use of two types of carbon and glass FRP sheets, and various parameters were examined, including the number of FRP layers and the strength of the concrete. The results demonstrated that the utilization of CFRP wrapping resulted in a higher ultimate load-bearing capacity compared to GFRP composites [7]. In another study by Pachideh et al., the performance of concrete-filled steel tube columns with FRP confinement under axial compressive loading was investigated. The results demonstrated increased load capacity and stiffness, highlighting their suitability for building construction and retrofitting purposes [8]. Pachideh et al. investigated the effect of temperature rise on Concrete-Filled Double Skin Tubular Steel Columns with different core shapes. The study found that circular cores were more prone to damage, whereas diamond-shaped cores exhibited higher initial stiffness and ductility. Fractures occurred diagonally at 500°C and horizontally at 700°C from the column base [9]. The seismic performance of concrete-filled double-skin steel tubular columns with different inner section shapes has been investigated by Pachideh et al. They found that columns with circular inner sections experienced more damage, while those with diamond-shaped inner sections exhibited greater stiffness and ductility. The column with a circular inner section demonstrated stable behavior and maintained a higher energy absorption capacity [10].

Kalavagunta et al. conducted a study on CFRP-reinforced edged channel columns under axial load. The results of their research revealed that the load-bearing capacity increased by up to 16.75% for the fully reinforced cross-section and up to 10.26% for web strengthening. However, it was also observed that the capacity of the columns decreased and sudden failure occurred due to delamination and detachment of the CFRP reinforcement [11]. Considering factors such as the number of layers and the spacing of CFRP sheets were studied by Sundrraja & Sivasankar [12]. It was shown that transverse fibers have a greater increase in stiffness, bearing capacity, and axial deformation than longitudinal fibers. In the experimental study done by Prabhu & Sundrraja, carbon fibers with different thicknesses and spacing were transversely wrapped around steel filled with concrete, and the stress-strain behavior and fracture modes were investigated. It was observed that as the CFRP strips increase, the buckling occurs in the fiber-less area and the number of layers is very effective in controlling the axial deformation of specimens [13]. In 2013, the effects of parameters such as the type of reinforcement and concrete, and the shape of the cross-section on the behavior of concrete-filled steel tube columns were investigated by Dong et al. They found that the use of CFRP on solid and hollow circular columns had a better effect than on square sections [14]. Deficient beams with primary One-side and two-side damages on the tensile flanges were studied by Yousefi et al. They found that two-side damage reduces bearing capacity more than one-side damage while one-side damage, in addition to reducing ultimate load, has also caused global buckling of the beam. CFRP strengthening restored the load reduction and was also effective in reducing beam buckling [15]. Ghaemdoust *et al.* conducted a study of damaged steel short-square columns in which the defect was considered horizontal and vertical to the corner and center of the column [16]. Also, defective short steel circular columns strengthened using CFRP studied by Karimian et al. Studies have shown that the defect will reduce the bearing capacity of steel columns and the defects increase axial deformation and local buckling in the column [17]. Buchanan et al. conducted a study on the buckling and slenderness ratio of cold-formed circular columns. In this experimental and numerical study, columns with different cross-sectional areas and lengths were studied and results were compared [18].

Earlier studies have demonstrated that the utilization of CFRP in column retrofitting significantly enhances column strength and ductility. However, further investigations are required to advance the application of CFRP sheets for confining defected long steel columns subjected to axial loads. This study aims to evaluate the compressive behavior of long steel CHS columns with deficiencies, as the majority of existing research has primarily focused on shorter and medium-length columns. Additionally, the FRP strengthening technique will be employed to cover the defected area, as damage to the steel surface directly impacts the ultimate load-bearing capacity and failure modes. Retrofitting methods can also be employed to strengthen existing steel columns, piles, and bridge piers. In this paper, defected slender columns were prepared both with and without CFRP strengthening and subjected to deficiencies at two different locations. Numerical investigations were conducted to explore the effects of parameters such as dimensions of damage and CFRP wrapping on the behavior of the columns. A structured and purposeful flowchart of the paper process is presented in Figure 1.

2- Materials and methods

In this study, a total of 15 columns were generated to examine the impacts of defects and strengthening techniques. Additionally, a control column was created without any damage for comparison. The defects were introduced both horizontally and vertically, among these, 8 columns were strengthened using CFRP sheets.

2- 1- Characteristics of selected CHS column

The selected CHS column is a steel cold-formed column. The geometrical and material properties of this column are summarized in Table 1. In this table parameters D, t, L, and λ are the outer diameter, wall thickness, length, and global slenderness ratio of the column respectively and parameters E, F_y, F_u, and ε_r are modulus of elasticity, yield stress, ultimate stress and rupture strain of the material of the selected column

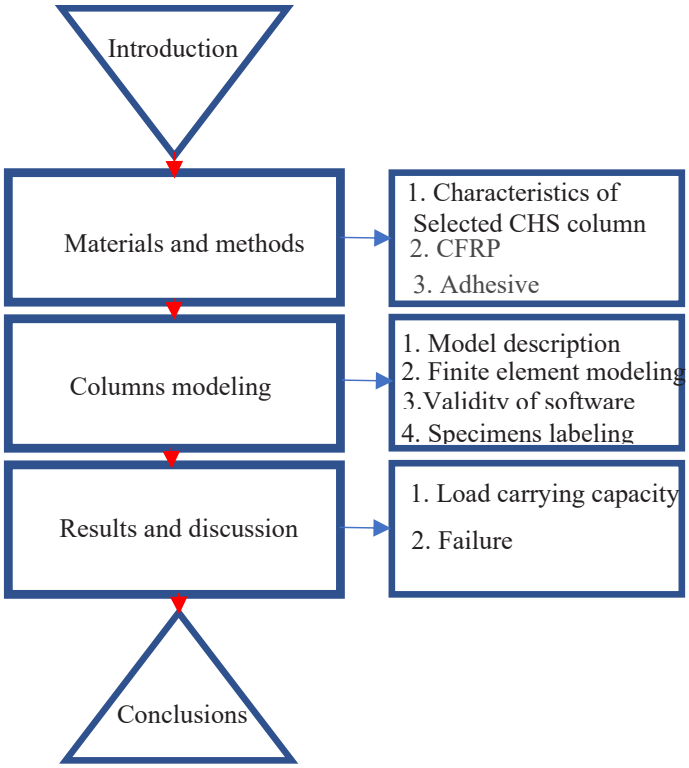

Fig. 1. Structured and purposeful flowchart of the essay process

Table 1. Sizes and properties of the CHS steel

D (mm)	t (mm)	L (mm)	λ	L/($\omega_0 + e_0$)	E (N/mm^2)	F_y (N/mm^2)	F_u (N/mm^2)	ε_r %
105.67	2.70	3083.0	1.02	1044	226,600	250	614	59.0

respectively. These parameters are as same as those used by Buchanan et al [18]. To create a deficiency, a horizontal or vertical notch was created at the middle of the section. These deficiency patterns are shown in Figure 2.

2- 2- CFRP

In this study, 4 layers of CFRP sheets (SikaWrap®230- C) with modulus of elasticity equal to 238000 MPa, Poisson ratio equal to 0.12, and thickness equal to 0.131 mm were used for strengthening of the deficient columns. The used CFRP fibers are unidirectional; the stress-strain curve behavior of CFRP is linear elastic up to the fracture and the specification of the CFRP materials is presented in Table 2.

2- 3- Adhesive

The adhesive used in this investigation which is Sikadur®330- epoxy is recommended by the CFRP product supplier. This adhesive is commonly used for CFRP (SikaWrap®230-K) where two resin and harder parts were mixed in a ratio of ۱:4, respectively. The Sikadur®330- epoxy has a modulus of elasticity of 4500 MPa and a 30 MPa tensile strength. The adhesive properties were retrieved from the conducted study by Karimian et al. [17] and the manufacturer of Sika [20]. Table 2 shows the adhesive properties used in this study.

Table 2. CFRP and adhesive specifications

Material	Thickness (mm)	Tensile Strength (MPa)	Modulus of elasticity (MPa)	Ultimate Strain (%)
CFRP (SikaWrap_-230 C) [20]	0.131	4300	238000	1.8
Adhesive (Sikadur_-330) [21]	0.869	30	4.5	0.9

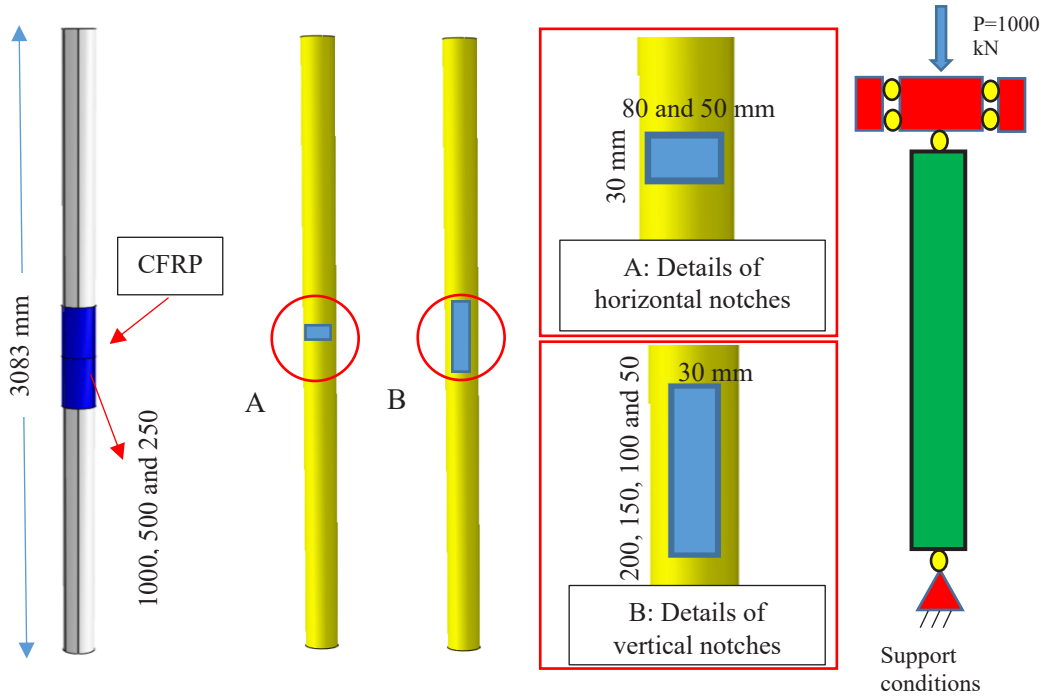

Fig. 2. A schematic view of strengthened and non-strengthened CHS steel section with longitudinal and transverse deficiency.

3- Column modeling

3- 1- Model description

To study the structural behavior of CHS steel sections strengthened with CFRP sheets, several finite element nonlinear models were prepared to be analyzed using ABAQUS software. For investigating deficiency effects and strengthening techniques, 15 columns were studied such as one non-deficient specimen as a control specimen , two columns with horizontal defects with 30 mm width, 50 and 80 mm length, four specimens with vertical defects with 30 mm width, and different lengths 50, 100, 150 and 200 mm. Figure 3 shows the support conditions, applied loads, and strengthening technique of the deficient column and three-dimensional finite element model which is developed by ABAQUS software. The applied load continued until the CHS columns reached to ultimate capacity.

3- 2- Finite element modeling

In order to investigate the structural behavior and the von Mises stresses at the cross-section thickness of CHS columns, especially at the damaged zone, all models were created using 20-node solid elements (C3D20R) with reduced integration. In FE modeling both nonlinear geometric and material analyses were considered.

All models were first imperfected and then were subjected to nonlinear analyses. To create imperfect models, two types of imperfection including local and global were considered. Global imperfection included two parts: (ω_0 + e_0) which is the combination of initial defect and centrifugal respectively and the fraction of effective length L / 1000. To apply local imperfections, the columns were first subjected to elastic buckling analysis and then the first two modes of elastic buckling analyses with imperfection values of t / 10 and t / 100 (t is cross-section thickness) were combined to create the imperfect model. For global imperfection, the value of ω_0 + e_0 was determined by equation (1) [21, 22, and 23]. In this equation E is Young's modulus, I is the second moment, N is the axial load, D is the mean of the outer diameter, ω is the lateral displacement of the middle column, ε_{max} and the ε_{min} are the maximum and minimum strains respectively. These values were obtained from the study carried out by Buchana et al, for the column 106×3-3080-P [18].

$$\frac{EI(\varepsilon_{max}-\varepsilon_{min})}{DN} - \omega = \omega_0 + e_0 \quad (1)$$

The 20-node (or Quadratic) 3D SOLID element and 5 mm mesh size and Tie method were also used to connect the adhesive and CFRP to the CHS steel column to generate the desired surface interaction. In analysis, loading continued until the specimens failed and the plastic strain was achieved. CFRP fibers were defined as linear and orthotropic in software because of their linear and unidirectional properties. Similar to the methods used in [17], adhesive properties were defined linearly. To achieve a modeling approach similar to the laboratory specimen, it is important to ensure that the simulation accurately represents the boundary conditions found in the laboratory. Based on the laboratory setup, all translational DOFs simulated the same as the experimental case. The boundary conditions were modeled by two

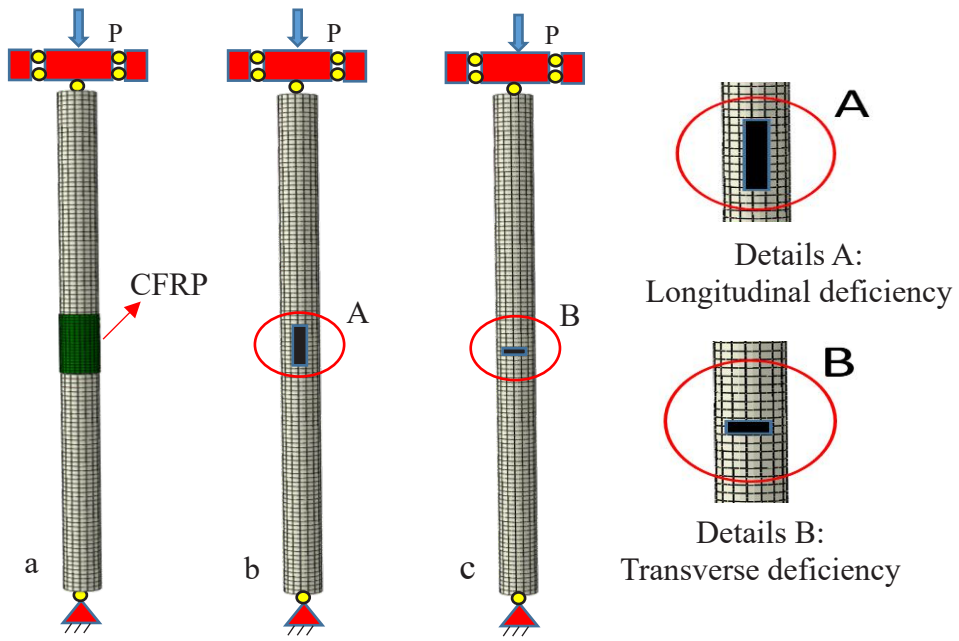

Fig. 3. A view of finite element modeling: (a) strengthened deficient specimen; (b) non-strengthened specimen with longitudinal deficiency (c) non-strengthened specimen with transverse deficiency

reference points one at each column end at the center of the cross section connected to the nodes of two ends by two rigid body constraints. Due to the axial displacement, the load was applied to the reference point at the loading edge (similar to the lab specimen test).

The Riks method, which is commonly used to predict the unstable behavior and geometrically nonlinear break fall of structures with nonlinear materials and boundary conditions, was implemented in this study. It was employed to conduct nonlinear analyses that precisely determined the failure modes and post-buckling behavior. Imperfect models were utilized for the analyses conducted under monotonic loadings, To achieve more realistic results.

3- 3- Validity of software results

Since, in FE analysis, the properties of the materials were defined nonlinearly, the modeling of the material was first verified base on coupon tests carried out by Buchanan [18]. Figure 4 shows the comparison between the numerical and experimental coupon test results. As this figure indicates there is a good agreement between the numerical and experimental results indicating the accuracy of FE modeling. To verify the accuracy of FE modeling of long steel columns, available experimental results provided in [18] were used, and numerical and relevant experimental results were compared in terms of section deformations, ultimate loads, failure modes, state of stress and strain in FE models. Table 1 summarizes the properties and geometry of the column Finite element modeling of column P-3-3080-106 tested in [18] which was used for verification. The mesh size affects the accuracy of the numerical results and the computational time. To determine the appropriate mesh size, the specimen was modeled with 3 mesh sizes, 0.01 m, 0.015 m, and 0.02 m. As Figure 5 indicates the precision of mesh sizes 0.01 m and 0.015 m are approximately the same. For the purpose of lower analysis time, mesh size of 0.015 m was chosen. Also, in Table 3, the differences in mesh size results are presented. In Figures 4 and 5, comparisons of the experimental and numerical results are shown. As these figures indicate there are good agreement between experimental and numerical results. CFRP and adhesive experimental and numerical modeling were conducted at previous works done by authors [15, 16 and 17].

3- 4- Specimens labeling

In the present study, totally 15 specimens were modeled including one non-defected column (control specimen, specimen NO.1), two defected but non-strengthened columns with different horizontal defect lengths (specimen NO.2 and specimen NO.3), four non-strengthened samples with different vertical defect length, and eight defected columns with different dimensions of strengthening. In all specimens, the defect width is constant and equal to 30 mm. Ultimate load of specimens was compared by the control column. For naming the models, the horizontal, vertical, defect size, and CFRP length are used. The horizontal parameters are represented by (H) and the vertical by (V). For specimen H-50-30-250, H is the horizontal defect, 50 is the defect length in millimeters, 30 is the defect width in millimeters, and last number is CFRP layer length. Specimen V-200-30, V is the vertical defect, 200 is defect length in millimeters, 30 is defect width in millimeters. This specimen is non-strengthened. The specifications of all columns are given in Table (4).

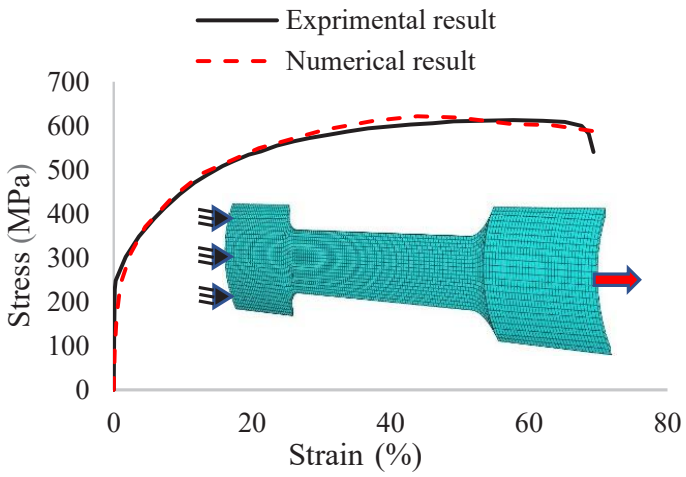

Fig. 4. Comparison between experimental engineering stress-strain curves of [18] and analytical results of 106×3-3080-P steel material for the case of monotonic loading

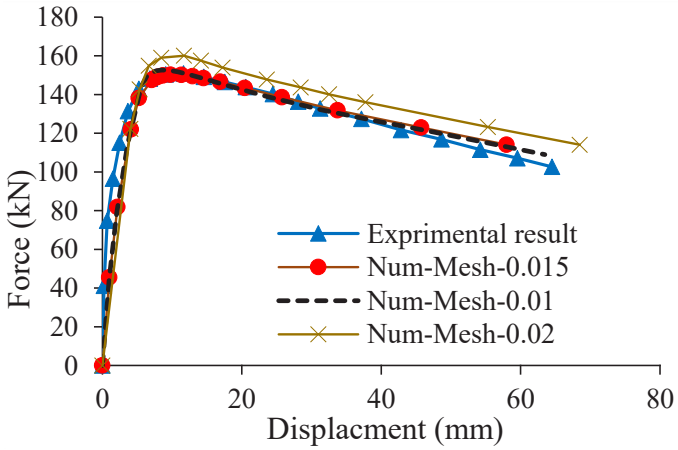

Fig. 5. Load-Displacement curves with different mesh sizes for experimental [19] and FE modeling of case 88.9×2.6-950-P

Table 3. The results of the validation chart

No	Specimen	Load bearing Capacity	
		Load (kN)	Increase/ decrease (%)
1	Control	150.2	-
2	Num-Mesh-0.015	151	+0.0053
3	Num-Mesh-0.01	151.1	+0.0059
4	Num-Mesh-0.02	158.6	+0.0558

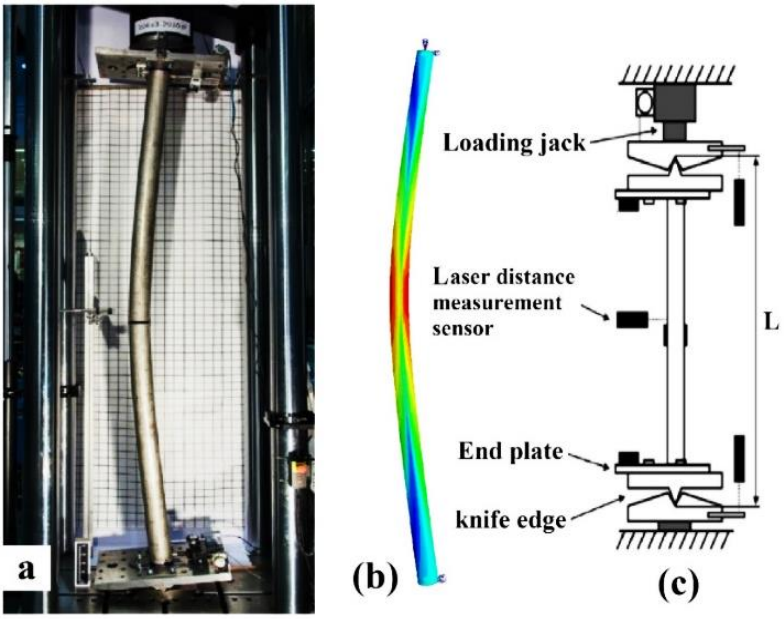

Fig. 6. Failure modes for the 106×3-3080-P specimen: a) Experimental [18], b) Numerical (this research), c) pin-ended long column test setup [18]

4- Results and discussion

4- 1- Load carrying capacity

In Table 4, the numerical results of strengthened and non-strengthened specimens are summarized. To investigate CFRP length and its influence on load-carrying capacity, three different CFRP lengths 250, 500, and 1000 mm were used for retrofitting. It should be noted that in this investigation, 4 layers of CFRP were used for retrofitting which was based on the recommendations presented in [17]. Table 4 presents the percentage of increase or decrease in the ultimate load of columns, compared to the control specimen. It illustrates the impact of horizontal damage (measuring 50 × 30 mm²) on column H-50-30, resulting in a 20% reduction in load-bearing capacity compared to the control column. Furthermore, when the damage dimensions were increased in column H-80-30, this reduction escalated to 52 percent. Figure 7 provides a visual comparison of the ultimate load of columns with horizontal defects. The figure demonstrates that an increase in damage dimensions leads to a decrease in both the initial stiffness and load-carrying capacity of the columns.

To address the created deficiency, various lengths of CFRP were employed for the repair. Figure 8 depicts the impact of these fibers on column stiffness and load-bearing capacity. As shown in the figure, the application of CFRP fibers to cover the damaged area resulted in a significant increase in both column stiffness and load-carrying capacity. For instance, specimen H-50-30-1000, retrofitted with 1000 mm CFRP fibers, exhibited an 18% higher load-carrying capacity compared to the control column and a 38% higher capacity compared to the defected column without retrofitting. As the objective of the study was to compensate for the damage and reduce the ultimate load, a CFRP length of 250 mm was chosen for the remaining specimens.

In Figure 9, a comparison is presented between horizontal and vertical defects. The columns labeled as H-50-30 and V-50-30, both having the same dimensions of 50 × 30 mm² for the damage area, exhibit ultimate loads of 120.5 kN and 140.2 kN, respectively. Despite having the same defect dimensions, the horizontal defect causes a greater reduction in the ultimate load compared to the vertical defect, with a 6.6% difference. This indicates that the horizontal defect is more critical and has a more significant impact on load reduction. It can be concluded that as the width of the defect decreases (the horizontal arc length of the circular column), the stiffness decreases more significantly, leading to faster failure of the column. Furthermore, considering the support conditions and global buckling at the middle of the column, a substantial reduction in stiffness and column strength occurs.

4- 2- Failure modes

In the present study, numerical analyses were conducted on slender circular columns subjected to axial compressive loading until reaching the ultimate load and plastic strain. When exposed to high compressive stresses, slender columns are prone to experiencing global buckling along their height, as opposed to local buckling observed in short columns. In the control column, initial failure manifested as global buckling accompanied by noticeable local deformations at the mid-height. As the loading progressed into the plastic range, the column underwent a secondary failure marked by mid-height local buckling (see Figure 6). For columns with horizontal deficiencies, the presence of a defected area accelerates the occurrence of failure, resulting in outward buckling on both sides of the defect, thereby reducing the width of the damaged area. Additionally, it is worth noting that columns with mid-height damage exhibit global buckling and bend in

Table 4. Specifications, deficiencies dimensions, and load-bearing capacities of the specimens

NO	Specimen	Deficiency			CFRP length (mm)	Load bearing Capacity	
		Length (mm)	Width (mm)	Position		Load (kN)	Increase/ decrease (%)
1	Control	N/A	N/A	N/A	N/A	150.2	-
2	H-50-30	50	30	Horizontal	N/A	120.5	-20
3	H-80-30	80	30	Horizontal	N/A	72.46	-52
4	H-50-30-250	50	30	Horizontal	250	154.85	+3
5	H-50-30-500	50	30	Horizontal	500	166.18	+10
6	H-50-30-1000	50	30	Horizontal	1000	177.78	+18
7	H-80-30-250	80	30	Horizontal	250	148.8	-1
8	V-50-30	50	30	Vertical	N/A	140.2	-6.6
9	V-100-30	100	30	Vertical	N/A	134.58	-10
10	V-150-30	150	30	Vertical	N/A	130.01	-13.3
11	V-200-30	200	30	Vertical	N/A	128.88	-14
12	V-50-30-250	50	30	Vertical	250	156.12	+3.9
13	V-100-30-250	100	30	Vertical	250	155.88	+3.7
14	V-150-30-250	150	30	Vertical	250	154.1	+2.5
15	V-200-30-250	200	30	Vertical	250	153	+1.8

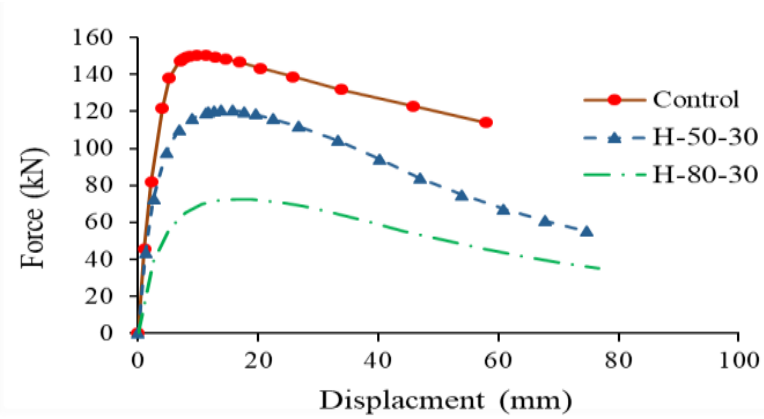

Fig. 7. Comparison of Load-Displacement curves for the control column and horizontal damaged column

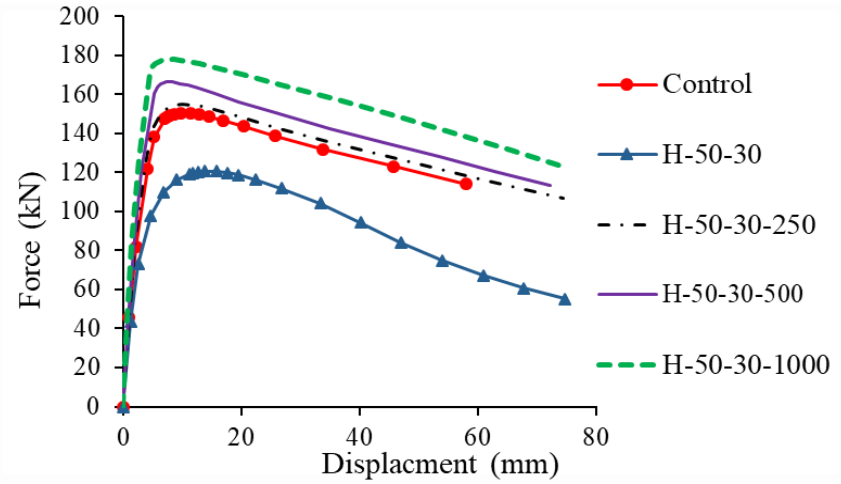

Fig. 8. Comparison of Load-Displacement curves for the control column and horizontal damaged column strengthened using CFRP

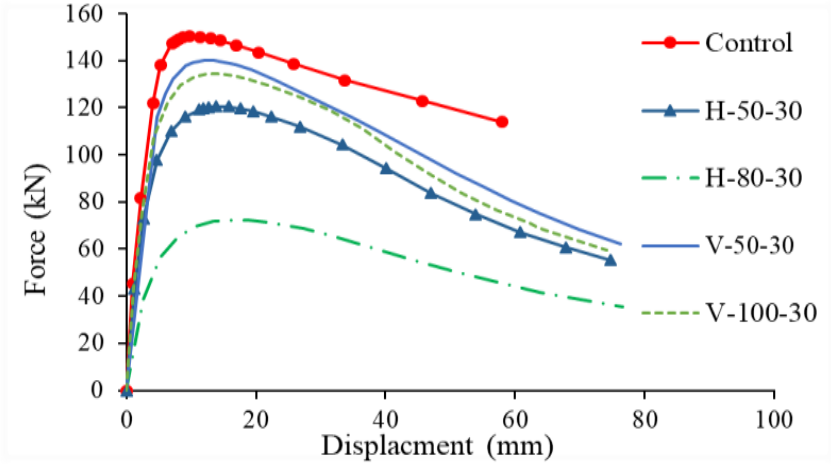

Fig. 9. Load-Displacement curves for horizontal damaged column and vertical damaged ones

the direction of the damage zone (see Figure 10-a). In the case of a non-strengthened column with a vertical notch, the application of load increases the cross-sectional damage area and subsequently leads to the occurrence of local buckling due to intensified stresses. Notably, the vertical defect tends to cause the edges of the notch to open (refer to Figure 10-b). Strengthening was performed using four layers of CFRP fibers. In the case of strengthened columns, CFRP significantly reduces stresses in the mid-column and delays the onset of local buckling at the defect zone. Figures 10-c and 10-d illustrate that the CFRP layers on the defect experience higher stress intensity and reach a plastic behavior.Top of Form

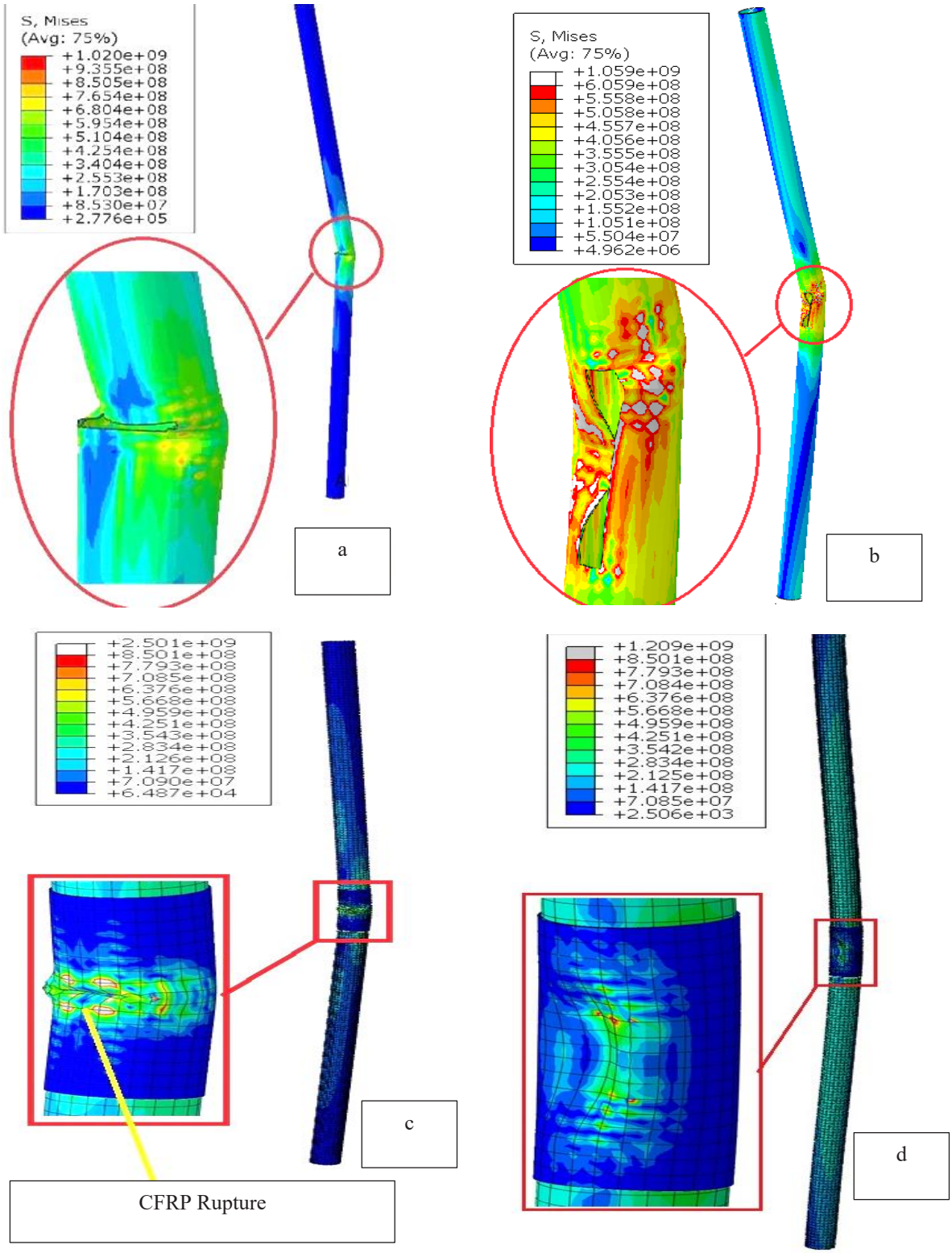

Fig. 10. Comparison of the Von Mises stress and failure modes in the specimens: (a) specimen H-80-30; (b) specimen V-200-30; (c) specimen H-80-30-250; (d) specimen V-200-30-250.

5- Conclusions

In this study, the analysis of several long-defected columns considering buckling and imperfections was conducted using ABAQUS software. The primary focus was on investigating the effects of CFRP fibers on defected long-circular steel columns. The modeling of the circular column involved initial buckling analysis to determine the buckling modes. Furthermore, nonlinear RIKS analysis and imperfection values were incorporated to analyze the post-buckling failure behavior. The steel column under investigation was cold-formed and had dimensions of 3083 mm in height, 105.67 mm in diameter, 2.70 mm in wall thickness, and a slender ratio of 1.02. Both vertical and horizontal notches were introduced in the column. The strengthening approach involved the use of four layers of CFRP. The research aimed to explore the effects of column defects on load capacity and the retrofitting of damaged zones to enhance the strength of long steel circular columns. A comparison was made among 15 columns with horizontal and vertical defects, leading to the following results:

In the column, a horizontal defect measuring 50 × 30 mm² was present in the middle of the member, leading to a 20% reduction in the load-bearing capacity of the long circular column. To address this deficiency, a repair strategy was implemented using four layers of CFRP. The CFRP strengthening method effectively delayed local buckling and reduced the intensity of stresses in the damaged zone.

Horizontal-defective columns exhibit a significantly lower load-bearing capacity compared to vertical-defective columns. For columns with the same dimensions of damage, specifically 50 x 30 mm², horizontal defects result in a 20% reduction in bearing capacity, whereas vertical notches lead to a 6% reduction. This discrepancy highlights the greater impact of horizontal defects over vertical defects. The results indicate that one of the reasons for the larger reduction in columns with horizontal defects is the extensive damage to a substantial portion of the column perimeter. Since the column is subjected to axial load, and global buckling primarily occurs in the middle of the column, it fails to demonstrate adequate structural performance. However, the use of CFRP fibers effectively delays buckling and appropriately increases the column's strength.

The failure mode of the control column is global buckling, with the focus being on the middle of the column. In the case of non-strengthened specimens with a horizontal defect, the failure mode is characterized by local buckling, specifically the shrinkage of notch edges. On the other hand, for specimens with a vertical notch, the failure mode involves the opening of defect edges. It is important to note that global buckling occurred in all columns. However, for strengthened specimens, stress concentration was observed around the area of the deficiency.

References

[1] Y. Chen, J. Wan, K. He, Experimental investigation on axial compressive strength of lateral impact damaged short steel columns repaired with CFRP sheets, Thin-Walled Structures, 131 (2018) 531-546.

[2] C. Huang, T. Chen, X. Wang, Compressive characteristics of damaged circular hollow section (CHS) steel columns repaired by CFRP or grout jacketing, Thin-Walled Structures, 119 (2017) 635-645.

[3] A. Cinitha, P.K. Umesha, N.R. Iyer, An overview of corrosion and experimental studies on corroded mild steel compression members, KSCE Journal of Civil Engineering, 18(6) (2014) 1735-1744.

[4] S. Sandrasekaran, T. Thilakranjith, M. Sundarraja, Axial behavior of CFRP jacketed HSS tubular members-an experimental investigation, 5 (2012) 1729-1737.

[5] Q.-L. Wang, Z. Zhao, Y.-B. Shao, Q.-L. Li, Static behavior of axially compressed square concrete filled CFRP-steel tubular (S-CF-CFRP-ST) columns with moderate slenderness, Thin-Walled Structures, 110 (2017) 106-122.

[6] K. Karimi, W.W. El-Dakhakhni, M.J. Tait, Behavior of Slender Steel-Concrete Composite Columns Wrapped with FRP Jackets, 26(5) (2012) 590-599.

[7] M. Touhari, R. Mitiche-Kettab, Behaviour of FRP Confined Concrete Cylinders: Experimental Investigation and Strength Model, Periodica Polytechnica Civil Engineering, 60(4) (2016) 647-660.

[8] G. Pachideh, M. Gholhaki, Evaluation of Concrete Filled Steel Tube Column Confined with FRP, 2 (2019) 2019.

[9] G. Pachideh, M. Gholhaki, A. Moshtagh, An Experimental Study on Cyclic Performance of the Geometrically Prismatic Concrete-Filled Double Skin Steel Tubular (CFDST) Columns, Iranian Journal of Science and Technology, Transactions of Civil Engineering, 45(2) (2021) 629-638.

[10] G. Pachideh, M. Gholhaki, A.J.J.o.T. Moshtagh, Evaluation, Impact of temperature rise on the seismic performance of concrete-filled double skin steel columns with prismatic geometry, 49(4) (2021) 2800-2815.

[11] S. Kalavagunta, S. Naganathan, K.N. Bin Mustapha, Proposal for design rules of axially loaded CFRP strengthened cold formed lipped channel steel sections, Thin-Walled Structures, 72 (2013) 14-19.

[12] M. Sundarraja, S. Sandrasekaran, Behaviour of CFRP jacketed HSS tubular members under compression - An experimental investigation, 39 (2012) 574-582.

[13] G. Ganesh Prabhu, M.C. Sundarraja, Behaviour of concrete filled steel tubular (CFST) short columns externally reinforced using CFRP strips composite, Construction and Building Materials, 47 (2013) 1362-1371.

[14] J.F. Dong, Q.Y. Wang, Z.W. Guan, Structural behaviour of recycled aggregate concrete filled steel tube columns strengthened by CFRP, Engineering Structures, 48 (2013)

532-542.

[15] O. Yousefi, K. Narmashiri, M. Ghaemdoust, Structural behaviors of notched steel beams strengthened using CFRP strips, Steel and Composite Structures, 25 (2017) 35-43.

[16] M.R. Ghaemdoust, K. Narmashiri, O. Yousefi, Structural behaviors of deficient steel SHS short columns strengthened using CFRP, Construction and Building Materials, 126 (2016) 1002-1011.

[17] M. Karimian, K. Narmashiri, M. Shahraki, O. Yousefi, Structural behaviors of deficient steel CHS short columns strengthened using CFRP, Journal of Constructional Steel Research, 138 (2017) 555-564.

[18] C. Buchanan, E. Real, L. Gardner, Testing, simulation and design of cold-formed stainless steel CHS columns, Thin-Walled Structures, 130 (2018) 297-312.

[19] Sika Warp -230 C. Product Data Sheet. Edition13/06/2006.

[20] Sika, Sikadur®330- Product Data Sheet [computer program]://irn.sika.com/en/solutions_products/construction-markets/sika-structural-strengthening-solutions/02a013/ 02a013sa09.html

[21] O. Zhao, L. Gardner, B. Young, Structural performance of stainless steel circular hollow sections under combined axial load and bending – Part 1: Experiments and numerical modelling, Thin-Walled Structures, 101 (2016) 231-239.

[22] Y. Huang, B. Young, Experimental investigation of cold-formed lean duplex stainless steel beam-columns, Thin-Walled Structures, 76 (2014) 105-117.

[23] O. Zhao, B. Rossi, L. Gardner, B. Young, Behaviour of structural stainless steel cross-sections under combined loading – Part I: Experimental study, Engineering Structures, 89 (2015) 236-246.

HOW TO CITE THIS ARTICLE

O. Yousefi, Numerical Investigation on Structural Behaviors of Deficient Steel CHS Long Columns Strengthened Using CFRP, AUT J. Civil Eng., 6(4) (2022) 509-520.

DOI: 10.22060/ajce.2023.22325.5825